

Self-stabilization of the biosphere under global change: a tutorial geophysiological approach

W. Von Bloh, A. Block & H. J. Schellnhuber

To cite this article: W. Von Bloh, A. Block & H. J. Schellnhuber (1997) Self-stabilization of the biosphere under global change: a tutorial geophysiological approach, *Tellus B: Chemical and Physical Meteorology*, 49:3, 249-262, DOI: [10.3402/tellusb.v49i3.15965](https://doi.org/10.3402/tellusb.v49i3.15965)

To link to this article: <https://doi.org/10.3402/tellusb.v49i3.15965>



© 1997 The Author(s). Published by Taylor & Francis.



Published online: 18 Jan 2017.



Submit your article to this journal [↗](#)



Article views: 44



View related articles [↗](#)



Citing articles: 15 View citing articles [↗](#)

Self-stabilization of the biosphere under global change: a tutorial geophysiological approach

By W. VON BLOH, A. BLOCK and H. J. SCHELLNHUBER*, *Potsdam Institute for Climate Impact Research (PIK), Telegrafenberg, P. O. Box 601203, D-14412 Potsdam, Germany*

(Manuscript received 6 June 1996; in final form 24 February 1997)

ABSTRACT

A 2-dimensional extension of the simple Lovelock-Watson model for geosphere-biosphere feedback is introduced and discussed. Our enriched version also takes into account various pertinent physical, biological, and civilisatory processes like lateral heat transport, species competition, mutation, germination, and habitat fragmentation. The model is used as a caricature of the Earth System, which allows potential response mechanisms of the biosphere to environmental stress (as generated, e.g., by global warming or anthropogenic land-cover change) to be investigated qualitatively. Based on a cellular automaton representation of the system, extensive calculations are performed. They reveal a number of remarkable and, partially, counter-intuitive phenomena: our model biosphere is able to control almost perfectly the geophysical conditions for its own existence. If the environmental stress exceeds certain thresholds, however, life breaks down on the artificial planet via a first-order phase transition, i.e., in a non-reversible way. There is a close connection between self-stabilizing capacity, biodiversity and geometry of habitat fragmentation. It turns out, in particular, that unrestricted Darwinian competition, which reduces the number of co-existing species, is the best guarantee for survival of the artificial ecosphere as a whole.

1. Introduction

Humanity's experiment in exploring the resilience of the Earth System to large scale perturbations (e.g., modification of atmospheric composition or fragmentation of terrestrial vegetation cover) is now in full gear. First results of this experiment (called Global Change) have already been achieved, in particular, statistical evidence for anthropogenic global warming and the erosion of biodiversity. A full account of the climatic aspects is provided by the forthcoming IPCC Report (Bolin et al. 1996); the present state of the biosphere is described, for instance, in Walter and Breckle (1991).

Unfortunately, the investigators here are probing their own material support system, which

cannot simply be replaced by a new specimen once the previous one has been worn out. The only way out this dilemma seems to be in modeling and computer simulation based on extensive non-destructive measuring and monitoring campaigns. The so-emerging virtual Earth Systems can be scrutinized safely in order to give deeper insights into the interactions of the various constituents and so avoid irreversible dead-end streets for the evolution of the original planet.

Big international research programmes like WCRP (WCRP 1994) and IGBP (IGBP 1994) are considered major stepping stones on our way towards such a fully-fledged Earth-System analysis. As a matter of fact, detailed 3D analogical models of the coupled geosphere-biosphere dynamics are supposed to transpire from these and related efforts within the next decade.

At present, such models are not yet available, but even when they exist they may be almost as

* Corresponding author.

difficult to handle as their real counterpart. Therefore it seems to be wise to keep on studying *caricatures* of the Earth System too, in the form of conceptual or even tutorial models (the different approaches to Earth-System modelling are discussed, e.g., in Schellnhuber 1996). Such a strategy is well-suited for uncovering qualitative phenomena and for exploring the topology, though not perhaps the geometry, of the system's phase space. The caricature may specifically reveal pertinent traits of the complex object under investigation and shatter conventional folklore based on conviction rather than analysis.

This modelling philosophy is further supported by recent insights of non-linear physics (Schuster 1989, Ott et al. 1994). They suggest looking for generic dynamical patterns of complex systems rather than striving for numerical predictions of details, which generally exhibit exponential sensitivity to conditional and computational errors. The identification of the major feedback mechanisms regulating or destabilizing the system in question is a crucial element of such a semi-quantitative analysis.

The evolution of the global ecosphere through billions of years was governed by the interaction of the biosphere and its geophysical environment as defined by the main factors insolation, plate tectonics, and the state of the atmosphere-hydrosphere system. A full explanation and reconstruction of the quaternary glaciation episodes, for example, seems to demand a thorough understanding of the planetary biogeochemical cycles as mediated by Life. The scientific paradigm behind these theories has been pioneered by J. Lovelock and his geophysiological approach to Earth-System analysis (Lovelock 1989, 1991).

A particularly useful ansatz for the investigation of geosphere-biosphere feed-backs is the Lovelock-Watson model (LWM) of "Daisyworld" (Watson and Lovelock 1982, Watson and Lovelock 1983). Despite its toy character, this model investigates possible mechanisms of environment stabilization through evolutionary adaption of terrestrial vegetation to varying insolation. We present here a 2D cellular automaton (CA) version of the original LWM, which takes into account a number of physical (e.g., lateral heat flow) and biological (e.g., competition and mutation) processes reflecting the dynamics within the real Earth System.

Our study has two main objectives, namely: (i) to mimic, on a tutorial level, the impacts of global change, like the modification of radiative forcing through anthropogenic emissions of greenhouse gases or man-made fragmentation of landscapes; (ii) to provide, on a conceptual level, potential building blocks for more sophisticated Earth-System models to be constituted in coming years.

Our material is organized as follows. In Section 2, we briefly review the original LWM. In Section 3, the extended model, which allows for infinitely many coexisting species, is introduced and discussed. The results of the quantitative analysis are presented in Section 4. In Section 5, the impacts of habitat fragmentation, i.e., the effects of heterogeneity, are analysed. The lessons to be learned from our geophysiological approach are summarized in the concluding section.

2. The original Daisyworld model

The familiar LWM is a zero-dimensional caricature of a planet, which is illuminated by the sun and which is able to support merely 2 different types of vegetation cover.

The surface of the "naked" planet, i.e., the planet without vegetation, is characterized by an overall albedo A_0 . The equilibrium temperature T_0 depends on the insolation S and the black body radiation according to

$$\sigma_B T_0^4 = S(1 - A_0), \quad (1)$$

where σ_B is the Stephan-Boltzmann constant. The biosphere consists of 2 components only.

- Species 1 with albedo $A_1 > A_0$ ("white daisies"), covering an area a_1 with temperature $T_1 < T_0$.
- Species 2 with albedo $A_2 < A_0$ ("black daisies"), covering an area a_2 with temperature $T_2 > T_0$.

The growth rate $\beta(T_i)$ of species i is a unimodular function with a maximum at $T_{\text{opt}} = 22.5^\circ\text{C}$:

$$\beta(T_i) = \begin{cases} \frac{4}{(40-5)^2} (T_i - 5)(40 - T_i), & 5 < T_i < 40, \\ 0, & \text{otherwise.} \end{cases} \quad (2)$$

The dynamics of the toy biosphere is governed by a system of 2 coupled nonlinear differential equations:

$$\begin{aligned} \dot{a}_1 &= a_1(\beta(T_1)x - \gamma), \\ \dot{a}_2 &= a_2(\beta(T_2)x - \gamma). \end{aligned} \tag{3}$$

Here γ denotes a constant mortality rate and x , the uncovered area, is trivially given by

$$x = 1 - a_1 - a_2. \tag{4}$$

For the sake of even more simplicity, the total area of the planet has been set equal to unity and the solar radiation is measured in "optimal insolation" units:

$$S' = S \frac{1 - A_0}{\sigma_B T_{opt}^4}. \tag{5}$$

This feedback system has been analysed by several authors (Isakari and Somerville 1989, Zeng et al. 1990, De Gregorio et al. 1992, Saunders 1994) in great detail. One remarkable result is that, in contrast to the uncovered planet, the "bioplanet" is able to hold the global temperature relatively constant when the external "control parameter" S is varied within a rather wide range. This property of self-regulation is referred to as "homeostasis". As a matter of fact, homeostasis is achieved here by a rather simple mechanism: white (black) daisies are fitter in hot (cold) climates as their comparatively high (low) albedo tends to reduce (increase) the local temperature.

Note that by conceiving σ_B as a function of the CO_2 concentration of the atmosphere, it is possible to take the greenhouse effect into account.

3. Introducing spatial dependence, competition, and mutation into Daisyworld

In general, the stable coexistence of many different species in Daisyworld can be brought about either by temporal fluctuations or by extending the spatial dimensionality. In this paper, the second approach is used and our planet will be represented by a 2D plane with coordinates x and y (Schellnhuber and Von Bloh 1994).

The "climate" here coincides with the temperature field $T(x, y, t)$, which is governed by an elementary energy balance equation (Henderson-

Sellers and McGuffie 1990):

$$\begin{aligned} C \frac{\partial T(x, y, t)}{\partial t} &= D_T \left(\frac{\partial^2}{\partial x^2} + \frac{\partial^2}{\partial y^2} \right) T(x, y, t) \\ &\quad - \sigma_B T(x, y, t)^4 + S(1 - A(x, y, t)), \end{aligned} \tag{6}$$

where D_T denotes the diffusion constant and $A(x, y, t)$ represents the spatiotemporal distribution of albedo. The latter reflects the prevailing vegetation pattern. The homogeneous solutions of eq. (6) are equivalent to the solutions of eq. (1) of the original LWM.

We consider an extended biosphere consisting of infinitely many different species, which may be conveniently classified by their specific albedos $A \in [0, 1]$. Hence, the variable A serves a 2-fold purpose, namely (i) to label the "daisies" stored in the genetic pool, and (ii) to express their radiative properties. As a consequence, the vegetation dynamics within our model can be directly represented by the albedo dynamics.

To achieve this, we have to translate the vegetation growth rules, which can be set up in the spirit of the LWM, into albedo modification rules. Their dependence on T and eq. (6) then determine the coevolution of albedo and temperature field in the plane. As the analytic solution of this intricate non-linear dynamics is unfeasible, we will have to resort to numerical computation schemes based on discretization of the system. It is therefore reasonable to employ the CA approach from the outset (Wolfram 1986, Goles 1994.) One major advantage of this approach is the fact that consistent albedo modification rules can be written down immediately.

The CA is constructed as follows: the plane is replaced by a quadratic lattice (x_i, y_j) , where $x_i = i \Delta x; y_j = j \Delta y; i, j \in \mathbb{N}$ and the basic spatial units $\Delta x, \Delta y$ can be chosen arbitrarily. Time proceeds in discrete steps $t_n = n \Delta t$, where $n \in \mathbb{N}$ and Δt is again an optional unit. Thus any systems variable F becomes a function $F(x_i, y_j, t_n)$.

The occurrence of vegetation in a particular cell (x_i, y_j) at time t_n can be indicated by a binary coverage function $c(x_i, y_j, t_n): \mathbb{N}^3 \rightarrow \{0,1\}$. The albedo dynamics is then determined by the following rules:

(1) $c(x_i, y_j, t_n) = 1$, i.e., the cell is covered by vegetation.

$$c(x_i, y_j, t_{n+1}) = \begin{cases} 1 & \text{with probability } 1 - \gamma, \\ 0 & \text{otherwise} \end{cases};$$

\Rightarrow

$$A(x_i, y_j, t_{n+1}) = \begin{cases} A(x_i, y_j, t_n) & \text{if } c(x_i, y_j, t_{n+1}) = 1, \\ A_0 & \text{otherwise.} \end{cases}$$

(7)

(2) $c(x_i, y_j, t_n) = 0$, i.e., the cell is uncovered.

Then choose at random a next-neighbour cell (x_{NN}, y_{NN}) of (x_i, y_j) and make the following distinction:

(a) $c(x_{NN}, y_{NN}, t_n) = 0$

\Rightarrow

$$c(x_i, y_j, t_{n+1}) = 0,$$

$$A(x_i, y_j, t_{n+1}) = A_0. \tag{8}$$

(b) $c(x_{NN}, y_{NN}, t_n) = 1$

$$c(x_i, y_j, t_{n+1}) = \begin{cases} 1 & \text{with probability } \beta, \\ 0 & \text{otherwise} \end{cases};$$

\Rightarrow

$$A(x_i, y_j, t_{n+1}) = \begin{cases} f(A(x_{NN}, y_{NN}, t_n)) & \text{if } c(x_i, y_j, t_{n+1}) = 1 \\ A_0 & \text{otherwise.} \end{cases} \tag{9}$$

Thus, γ and β again denote mortality and growth rate per each time step t_n , respectively. Regarding the functional dependence of the growth probability on the spatial distribution of temperature, two obvious choices can be made:

(A) β depends only on the temperature of the uncovered cell at point (x_i, y_j) , i.e.,

$$\beta = \beta(T(x_i, y_j, t_n)). \tag{10}$$

(B) β is determined by the temperature of the next-neighbour cell (x_{NN}, y_{NN}) , i.e.,

$$\beta = \beta(T(x_{NN}, y_{NN}, t_n)). \tag{11}$$

Hence in the first version, (A), the growth rate depends on the state of the area that will be covered by the vegetation in the next time step, while in the second version, (B), the temperature of the vegetation patch which initiates the growth determines the growth probability. It turns out that this innocent-looking local distinction induces

rather different behaviour even at the systems scale (see below).

The function f in (9) offers the opportunity to incorporate also more sophisticated biological effects: by choosing, for instance,

$$f(A) = A + R, \tag{12}$$

where R is a random number distribution with the properties

$$R \in [-r, r], \quad \langle R \rangle = 0, \tag{13}$$

it is possible to take mutations of the albedo into account. Here $r \geq 0$ can be interpreted as the mutation rate.

The CA is completed by solving the temperature evolution eq. (6) by an explicit finite-difference scheme on the square lattice with the same resolution as employed for the growth dynamics. The discretization step must be chosen in the way that the stability of the explicit scheme is guaranteed and no bifurcation (as, e.g., in the logistic map) takes place. A list of the chosen parameter settings is shown in Table 1. These values are used unless stated otherwise.

3.1. Comparison with the original model

Our extended geophysiological model for biosphere-geosphere interactions contains all the dynamics of the zero-dimensional LWM as a special subprocess. To demonstrate this, we have to consider the true evolution of the vegetation density N . Within the discrete CA formalism, N is defined as follows:

$$N(x_i, y_j, t_n) := \langle c(x_i, y_j, t_n) \rangle, \tag{14}$$

Table 1. List of the values assigned to the adjustable parameters in all computer simulations referred to in this paper

Parameter	Value
σ_B	$5.6696 \cdot 10^{-8}$
D_T	500
C	2500
A_0	0.5
γ	0.02
Δt	1
Δx	1
Δy	1

where $\langle \cdot \rangle$ denotes an averaging over a statistical ensemble. Thus $N(x_i, y_j, t_n)$ represents the probability of encountering vegetation of any type in cell (x_i, y_j) at time t_n . The dynamics of N is implicitly determined by the rules summarized in eqs. (7) to (9).

To simplify the calculations, we restrict the vegetation to 1 species in 2 spatial dimensions without considering mutations ($f(A)=A$). We have:

$$\begin{aligned}
 N(x_i, y_j, t_n + \Delta t) = & (1 - \gamma)N(x_i, y_j, t_n) + \beta(T) \\
 & \times (1 - N(x_i, y_j, t_n)) \\
 & \times \frac{1}{4} \{N(x_i + \Delta x, y_j, t_n) + N(x_i - \Delta x, y_j, t_n) \\
 & + N(x_i, y_j + \Delta y, t_n) + N(x_i, y_j - \Delta y, t_n)\} \\
 & + N(x_i, y_j, t_n) \quad (15)
 \end{aligned}$$

The next step is to take the continuous limit by making a Taylor expansion in Δx , Δy , and Δt up to 2nd order in space and 1st order in time, which results in the following expressions:

$$\begin{aligned}
 N(x_i \pm \Delta x, y_j, t_n) = & N(x_i, y_j, t_n) \pm \Delta x \frac{\partial N}{\partial x} \\
 & + \frac{1}{2} \Delta x^2 \frac{\partial^2 N}{\partial x^2} + O(\Delta x^3),
 \end{aligned}$$

$$\begin{aligned}
 N(x_i, y_j \pm \Delta y, t_n) = & N(x_i, y_j, t_n) \pm \Delta y \frac{\partial N}{\partial y} \\
 & + \frac{1}{2} \Delta y^2 \frac{\partial^2 N}{\partial y^2} + O(\Delta y^3),
 \end{aligned}$$

$$\begin{aligned}
 N(x_i, y_j, t_n + \Delta t) = & N(x_i, y_j, t_n) + \Delta t \frac{\partial N}{\partial t} + O(\Delta t^2). \quad (16)
 \end{aligned}$$

Substituting the approximations in eq. (15) and performing some transformations, the following PDE can be obtained for growth version A, if we neglect the terms of higher order:

$$\begin{aligned}
 \frac{\partial N}{\partial t} = & -\gamma'N + \beta'(T)(1 - N) \\
 & \times \left\{ N + D_x \frac{\partial^2 N}{\partial x^2} + D_y \frac{\partial^2 N}{\partial y^2} \right\}, \quad (17)
 \end{aligned}$$

where $\gamma' = \gamma/\Delta t$, $\beta' = \beta/\Delta t$, $D_x = \frac{1}{2}\Delta x^2$, and $D_y =$

$\frac{1}{2}\Delta y^2$. In order to have a non-vanishing diffusion for low values of Δx , Δy , β must be enlarged. This can be compensated by a lower value of Δt , which ensures also the stability of the discretization scheme.

For growth version B, the density N is determined by:

$$\begin{aligned}
 N(x_i, y_j, t_n + \Delta t) = & (1 - \gamma)N(x_i, y_j, t_n) \\
 & + (1 - N(x_i, y_j, t_n)) \\
 & \times \frac{1}{4} \{ \beta(T(x_i + \Delta x, y_j, t_n))N(x_i + \Delta x, y_j, t_n) \\
 & + \beta(T(x_i - \Delta x, y_j, t_n))N(x_i - \Delta x, y_j, t_n) \\
 & + \beta(T(x_i, y_j + \Delta y, t_n))N(x_i, y_j + \Delta y, t_n) \\
 & + \beta(T(x_i, y_j - \Delta y, t_n))N(x_i, y_j - \Delta y, t_n) \}. \quad (18)
 \end{aligned}$$

The resulting PDE for N is

$$\begin{aligned}
 \frac{\partial N}{\partial t} = & -\gamma'N + (1 - N) \\
 & \times \left\{ \beta'N + \left(D_x \frac{\partial^2}{\partial x^2} + D_y \frac{\partial^2}{\partial y^2} \right) (\beta'N) \right\}. \quad (19)
 \end{aligned}$$

Let us emphasize here that for homogeneous solutions, i.e., $N(x, y, t) \equiv N(t)$, the eqs. (15) and (18), respectively, are identical to the zero-dimensional LWM for one species (see eq. (3)).

If we include mutations of the albedo according to (12) for the homogeneous solution $N(A; t)$ we get:

$$\begin{aligned}
 N(A; t_n + \Delta t) = & (1 - \gamma)N(A; t_n) + \beta(T) \\
 & \times \left(1 - \int_0^1 N(A'; t_n) dA' \right) \frac{1}{2r} \int_{A-r}^{A+r} N(A'; t_n) dA'. \quad (20)
 \end{aligned}$$

A Taylor expansion in A yields the following expression for $N(A + \Delta A; t_n)$:

$$\begin{aligned}
 N(A + \Delta A; t_n) = & N(A, t_n) + \Delta A \frac{\partial}{\partial A} N(A; t_n) \\
 & + \frac{1}{2} \Delta A^2 \frac{\partial^2}{\partial A^2} N(A; t_n) + O(\Delta A^3). \quad (21)
 \end{aligned}$$

Inserting (21) into (20) and taking the continuous limit in t , the following equation, valid for small

mutation rates r , is obtained:

$$\begin{aligned} \frac{\partial}{\partial t} N(A;t) &= -\gamma'N(A;t) + \beta'(T) \\ &\times \left(1 - \int_0^1 N(A';t)dA' \right) \\ &\times \left(N(A;t) + \frac{1}{6} r^2 \frac{\partial^2}{\partial A^2} N(A;t) \right). \end{aligned} \tag{22}$$

This analysis can be expanded to all aspects of our full CA to demonstrate that the discretization preserves the right physics and biology.

4. Results

The dynamics of the extended geophysiological model introduced in the previous section is integrated numerically. We present here results of extensive investigations performed on a powerful parallel computer (IBM SP2). In general, the cellular automaton was implemented on finite 2D-lattices (200×200) with periodic boundary conditions. It should be mentioned that all the following results have been achieved using model B, i.e., the growth probability depends on the temperature according to eq. (11).

4.1. Equilibrium behaviour

Let us first choose a fixed insolation well within the range where the biosphere is able to maintain optimal subsistence conditions. Let us assume, for instance, that $S' = 1$, implying $T_0 = T_{opt}$. We vary, however, the mutation rate r in order to reveal the relations between mutation, biodiversity, and adaptive capacities.

The system is initialized by a random distribution of vegetation (albedo): then the rules of the cellular automaton are applied. After approximately 10^4 iterations, the global average temperature approaches the optimum growth temperature T_{opt} , i.e., the system has relaxed to a statistical equilibrium. Further iterations produce significant *local* fluctuations but do not modify the mean properties of the model planet. Fig. 1 depicts a typical equilibrium distribution of species (characterized by their albedo) and the associated two-dimensional temperature field.

The species spectrum $B(A)$ is defined as follows: $B(A)dA :=$ number of species with albedo A'

$$\in [A, A + dA]. \tag{23}$$

Note that due to the finiteness of the lattice we have only finitely many “daisies” on our planet; therefore this and the following quantities are well defined. The mean albedo \bar{A} of our model biosphere and its variance σ^2 are then given by

$$\bar{A} = \frac{1}{B} \int_0^1 AB(A)dA, \tag{24}$$

$$\sigma^2 = \frac{1}{B} \int_0^1 A^2B(A)dA - \bar{A}^2, \tag{25}$$

where $B = \int_0^1 B(A)dA$ is the total “biomass”.

The variation of the species spectrum as a function of the mutation rate r is depicted in Fig. 2 for version B of the automaton. Extensive computations corroborate the fact that $B(A)$ can be approximated by a Gaussian distribution for $r < 0.1$, i.e.,

$$B(A) \propto e^{-(A-\bar{A})^2/2\sigma^2}. \tag{26}$$

The mean albedo \bar{A} consistently turns out to equal the optimum albedo A_{opt} , which is determined by

$$S(1 - A_{opt}) = \sigma_B T_{opt}^4. \tag{27}$$

Hence, we have

$$\bar{A} = A_{opt} = A_0 = 0.5, \tag{28}$$

if the natural choice for A_0 is made.

From Fig. 2, we can also see that σ is a monotonically increasing function of r . Without mutation ($r = 0$) the spectrum actually collapses into a δ -function at $A = A_{opt}$ if we take the limit for an infinite lattice size, while for large r an almost uniform spectrum emerges.

Fig. 3 reproduces the quantitative relationship between σ and r for fixed $S' = 1$. The saturation effect here can be explained easily: the uniform spectrum $B(A) \equiv 1$, where each species has the same ecological weight in Daisyworld, implies an upper limit for the variance, namely

$$\sigma^2 = \int_0^1 A^2 dA - \left(\int_0^1 A dA \right)^2 = \frac{1}{12}. \tag{29}$$

The dashed horizontal line in Fig. 3 marks the value $\sigma = \sqrt{1/12} = 0.28\dots$

4.2. Homeostatic response to increasing insolation

A particularly interesting question is the following: does the extended 2D Daisyworld model react

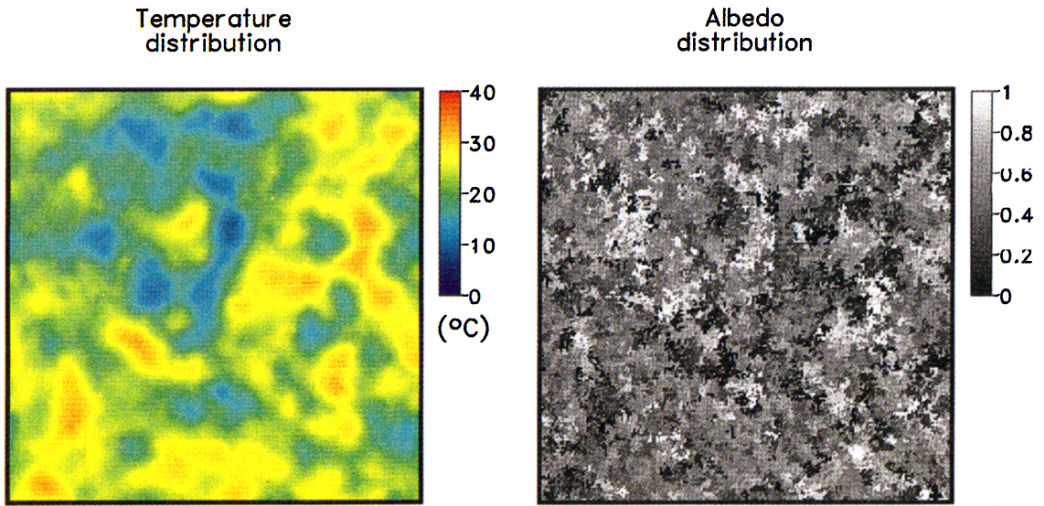


Fig. 1. Daisyworld in statistical equilibrium for $S' = 1$: snapshot of typical albedo distribution (right) and associated spatial temperature fluctuations around T_{opt} (left, in false colour representation).

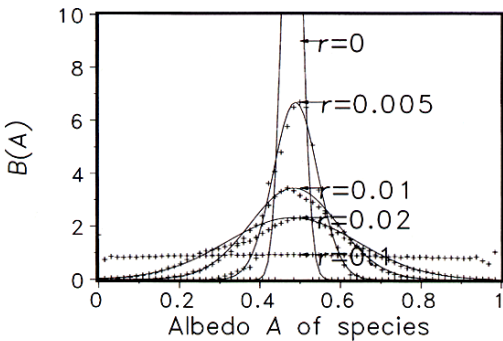


Fig. 2. Species spectra after 10^6 iterations for optimal constant insolation ($T_0 = T_{opt}$) and for different mutation rates $r = 0.0, 0.005, 0.01, 0.02$, and 0.1 , respectively. The solid curves represent the appropriate Gaussian fits. Note that the curve for $r = 0$ becomes a pure δ -function only in the limit of infinite lattice.

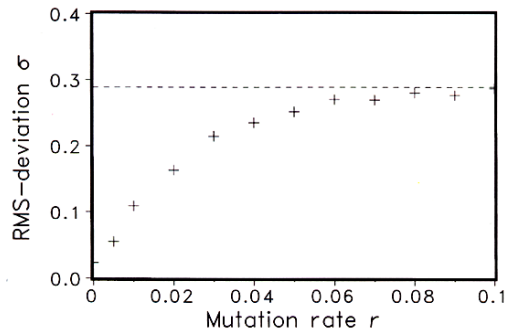


Fig. 3. Root-mean-square deviation σ of species spectra as a function of mutation rate r .

in a similar way to external perturbations (as variations of S') as the simple LWM? We generate the answer by simulating the system behaviour under quasistatic increase of the insolation. This is again done for different mutation rates r , which heavily influence the adaptive power of our model biosphere.

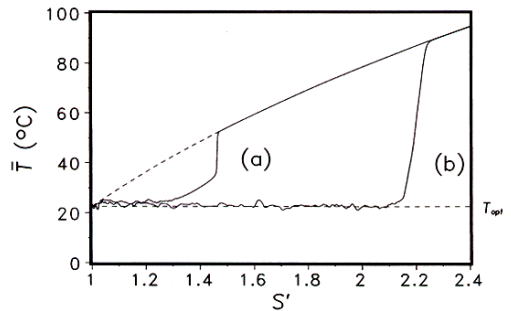


Fig. 4. Global mean temperature \bar{T} versus insolation S' for $r = 0$ (a) and $r = 0.01$ (b). The curved dashed line indicates the planetary temperature without life.

Fig. 4 demonstrates how the global mean temperature \bar{T} evolves with the modification of S' . Note that a moderate mutation rate ($r = 0.01$, curve b) significantly extends the homeostatic

effect as compared to the case without mutation (curve a).

Our general finding is that the extended model is an even better self-regulator than the simple LWM. The wiggles around the optimal control line $\bar{T} = T_{opt}$ are finite-size effects which will disappear on an infinite lattice. As mentioned above, however, the dependence of self-stabilizing behaviour on mutation is quite massive: for $r=0$, the critical insolation for vegetation breakdown is given by $S'_{crit} = 1.47$, while for $r=0.01$ the critical value has increased to 2.19!

We generalize these observations by calculating S'_{crit} as a function of r . The result is shown in Fig. 5, which clearly reveals the existence of an optimum mutation rate $r_{opt} \approx 0.06$. The associated maximum critical insolation strength is given by $S'_{crit} = 2.41$.

The different realizations A and B (see eqs. (10) and (11) for the CA growth rules result in rather distinct responses to increasing insolation. This is demonstrated in Fig. 6, which contrasts the evolution of \bar{T} with growing S' and identical $r=0.05$ for the 2 versions. We observe that the critical insolation in case A is significantly smaller than in case B.

Of course, the increase of S' heavily influences the species spectrum which adjusts in a self-stabilizing way. As a matter of fact, the rms-deviation σ significantly decreases when the sun becomes brighter (or the greenhouse gases accumulate). In other words, adaptation to non-optimal environmental conditions implies loss of biodiversity. Fig. 7 depicts the species spectra asso-

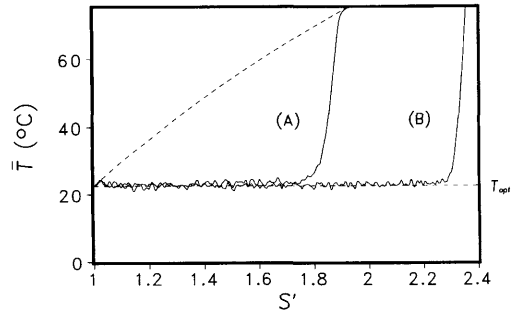


Fig. 6. Global mean temperature \bar{T} versus insolation S' for version A and B, respectively, of the CA growth rules (mutation rate $r=0.05$).

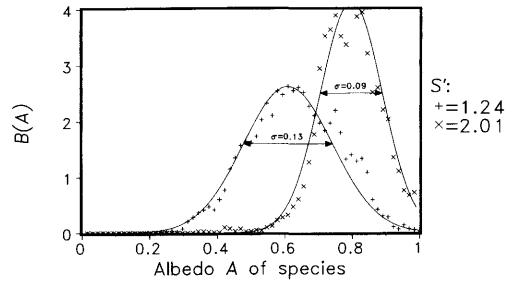


Fig. 7. Species spectra for $S' = 1.24$ and 2.01 , respectively; $r=0.01$.

ciated with two different values of S' and identical mutation rate.

The dwindling of biodiversity can be explained analytically, if we inspect the behaviour of β as a function of $T - T_{opt}$. Local energy balance implies

$$T - T_{opt} = [S(1 - A)/\sigma_B]^{1/4} - [S(1 - A_{opt})/\sigma_B]^{1/4} \\ = \text{const.} \times (S')^{1/4} [(1 - A)^{1/4} - (1 - A_{opt})^{1/4}]. \quad (30)$$

Linearization of the term in square brackets yields

$$T - T_{opt} \approx \text{const.} \times (S')^{1/4} (A_{opt} - A), \quad (31)$$

in the neighbourhood of optimum albedo A_{opt} which is itself a strictly increasing function of the insolation S . From the latter equation it becomes clear that a fixed deviation Δ from the optimal albedo, i.e., $|A - A_{opt}|(S')^{1/4} = \Delta > 0$, is punished the more severely the larger S' grows: $|T - T_{opt}|$ increases monotonically with S' and the growth probability β is a unimodal function with unique maximum at $T = T_{opt}$. So for higher $S' > 1$, species have to possess a closer-to-optimum albedo in

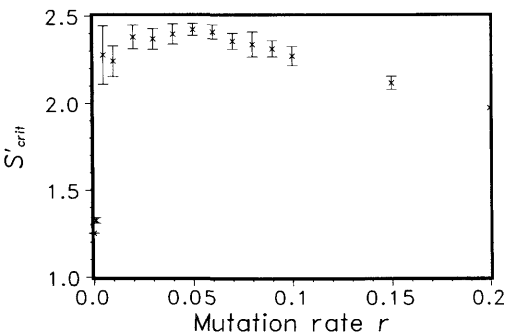


Fig. 5. Upper-limit insolation S'_{crit} for biosphere homeostasis as a function of mutation rate r . All values result from averaging over 10 different simulations; the error bars are included.

order to exhibit comparable fitness. As a consequence, the spectrum becomes steeper and steeper with growing insolation.

4.3. Hysteresis of life

Let us emphasize here that the break-down of the self-organized biosphere, which takes place when S' crosses the threshold S'_{crit} , is a clear cut first-order phase transition. Therefore hysteretic behaviour can be observed, i.e., the state of the system depends on its history.

We want to demonstrate this by forcing our extended Daisyworld through a full hysteresis loop. So S' will be quasi-statically increased from the optimal value 1 to a supercritical value, thereby destroying all vegetation. Thereafter, S' will be decreased down to the initial value to give the biosphere a chance for renaissance. But note that the planet cannot be recolonized by life if all species have been wiped out together with their seeds.

Let us therefore introduce a uniform stochastic background process, which represents the relentless germination of seeds protected by the soil. This can be achieved by slightly modifying the CA growth rules. Let us assume that $c(x_i, y_j, t_n)$ and all neighbouring cells are equally devoid of vegetation. Then instead of applying eq. (8), we make the following prescription:

$$c(x_i, y_j, t_{n+1}) = \begin{cases} 1 & \text{with probability } \pi \\ 0 & \text{otherwise} \end{cases},$$

$$A(x_i, y_j, t_{n+1}) = \begin{cases} \rho & \text{if } c(x_i, y_i, t_{n+1}) = 1 \\ A_0 & \text{otherwise} \end{cases}. \tag{32}$$

Here π is a very small number and ρ is a random variable with uniform distribution in the interval $[0,1]$. The germination process does not disturb the original dynamics of the system.

Fig. 8 shows what happens under these conditions, when S' rises and falls again: both the evolution of the global mean temperature and of the total vegetated area are depicted. For fixed $r=0.01$, recolonization of the planet starts when the insolation drops to $S'=1.25$. This is significantly smaller than the extinction value $S'=2.19!$ So, once the "point of no return" has been passed, it takes a great deal of effort to reinstall appro-

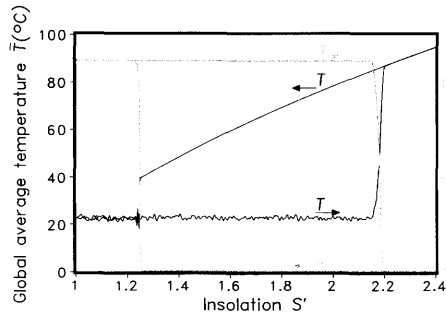


Fig. 8. Hysteresis diagram for the global mean temperature \bar{T} and the total vegetation area a in response to variation of S' . The arrows pointing to the right indicate increasing, the arrows pointing to the left decreasing insolation; $r=0.01$, $\pi=10^{-4}$.

priate conditions for the self-organized reappearance of the biosphere.

5. The impacts of fragmentation

Within our 2D model, the disposable area for vegetation growth is the full square, i.e., a simply connected domain. In the real world, however, the area available for biospheric adaption to global change forces is highly fragmented by civilisatory activities: urban settlements, infrastructures, agriculture, tourism, etc. The implications of habitat fragmentation on biodiversity is at present a much-debated issue.

Our toy planet constitutes an ideal theatre for investigating this and related questions in some depth; we specifically ask how the species spectrum and the resulting homeostatic properties of the biosphere depend on landscape heterogeneity. The latter is simulated here in a well-defined way: we employ the percolation model from solid state physics (Stauffer 1985) in order to simulate successive non-trivial reduction of growth space.

The percolation model on a square lattice is formulated in the following way: for a given probability $p \in [0, 1]$, each site will be randomly occupied with probability p . As a consequence, it will remain empty with probability $1-p$. A connected group of occupied sites is called a "cluster". The size of the clusters clearly grows with increasing p . "Percolation" is said to set in when the largest cluster extends from one end of the system to the other ("spanning cluster"). In the limit of

infinitely large lattices there exists a sharp threshold value $p_c = 0.59273 \dots$ for percolation. The spanning cluster associated with this phase transition is a multiple-connected fractal object with a power-law hole-size distribution. Fig. 9 gives an example of such a critical configuration which allows to traverse the entire lattice via next-neighbour steps.

Therefore, we have to distinguish between 3 qualitatively different regimes determined by the occupation probability:

- (1) $0 \leq p \leq 1 - p_c$: the collection of occupied sites does not form any spanning cluster, but the collection of unoccupied sites represents a connected "void space".
- (2) $1 - p_c < p \leq p_c$: neither the occupied nor the void sites form a connected structure.
- (3) $p_c \leq p \leq 1$: the collection of occupied sites does form a connected structure, but the void space is now disconnected.

We introduce civilisatory land-use into our extended Daisyworld by gradually diminishing the potential growth area in the following way: choose a (small) generating probability p_0 . In every time step, n all cells within the finite lattice are considered one by one and excluded from the growth space with probability p_0 . At time t_n , the probability that any specific site has been "civilized" is therefore given by

$$p(t_n) = 1 - (1 - p_0)^n. \quad (33)$$

Note that

$$1 - p(t_n) = (1 - p_0)^n \quad (34)$$

is then the statistical fraction of habitable area after n time steps.

Our fragmentation scheme is independent of the actual status of the cell under consideration. Furthermore, all physical properties, such as diffusive heat transport remain unaffected. We now present some computer simulation results,

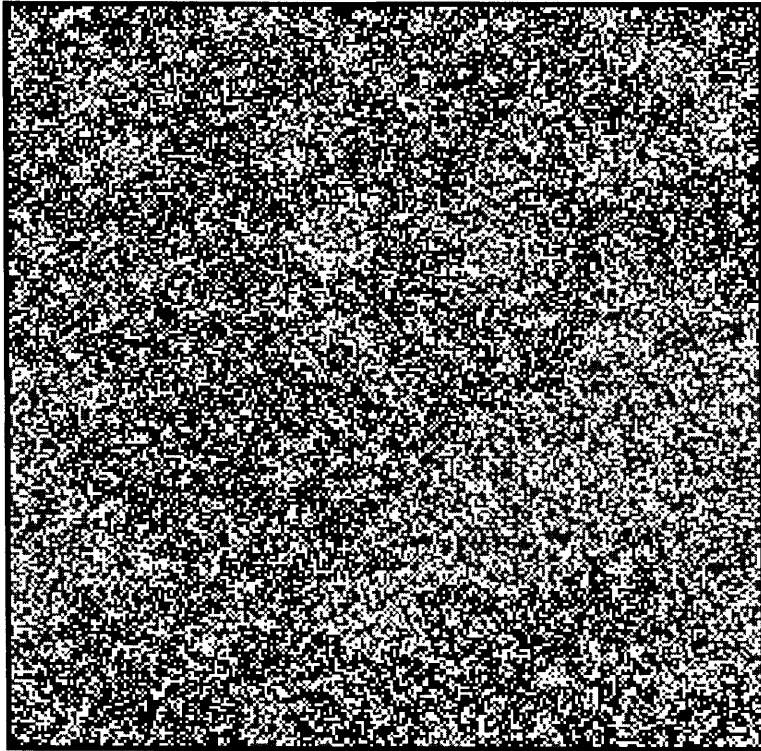


Fig. 9. Patch-work of occupied sites in the standard percolation model at criticality ($p = p_c = 0.5973, \dots$). The fractal spanning cluster is marked by the darker shade. Lattice size is 100×100 .

which shed light on the systems behaviour of "anthropomorphic Daisyworld".

First, we test the decay of self-stabilizing power with increasing patchiness parameter $p(t_n)$, i.e., for growing n . For fixed S' and $p_0 = 1.23 \cdot 10^{-6}$, we perform $n = 2 \cdot 10^6$ time steps, to destroy almost ($\approx 91.3\%$) all growth sites. Fig. 10 reproduces our findings regarding the relation between global mean temperature \bar{T} and the percolation parameter p . We observe that even the fragmented biosphere is able to stabilize the planetary temperature near the optimal value, unless p exceeds a value of approximately 0.4.

Our numerical results are robust. A series of extensive calculations with increasing lattice dimensions shows that finite-size effects can be neglected: the homeostatic response of the biosphere to fragmentation results in a well-defined p - \bar{T} -curve for any fixed S' (see Fig. 11).

As a matter of fact it turns out that the above-mentioned threshold value for patchiness has universal character, i.e., the behaviour depends neither on the system size nor the parameter settings. In particular, the strength of the insolation, which represents an external driving force, does not affect the threshold value. This is demonstrated in Fig. 12, where the self-organized mean temperature \bar{T} is plotted as a two-dimensional surface over the control space spanned by the driving-force variables T_0 (i.e., S') and p . The adaptive power of Daisyworld clearly breaks down when p approaches the value

$$\hat{p} := 1 - p_c \approx 0.407. \tag{35}$$

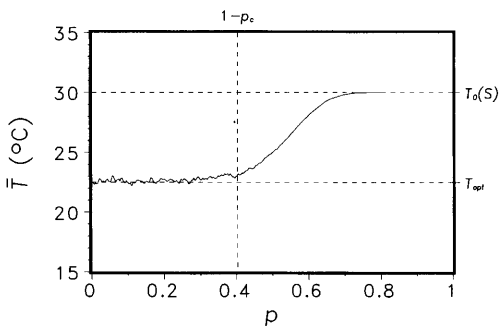


Fig. 10. Dependence of global mean temperature \bar{T} on the fragmentation parameter p . S' corresponds to 30°C for the temperature $T_0(S')$ of the "dead" planet. The broken vertical line at $p = 1 - p_c$ indicates the disconnection threshold for the habitable space.

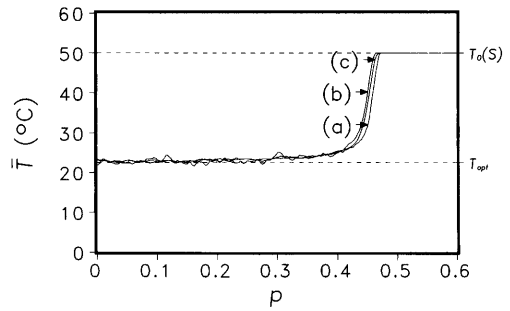


Fig. 11. Convergence of numerical results for p - \bar{T} relationship for increasing lattice size, (a) 200×200 , (b) 400×400 , (c) 800×800 . S' has been fixed to a value generating a geophysical planetary temperature $T_0(S') = 50^\circ\text{C}$.

The explanation for this phenomenon is simple but illuminating: for $p > \hat{p}$ the growth space has lost its connectivity and is broken up into many isolated domains. Our toy model hence provides us with clear-cut evidence that the ecological performance of a system directly depends on its topology!

5.1. Fragmentation and biodiversity

In order to study the impacts of fragmentation on the abundance of different species in Daisyworld we keep $S' = 1$ fixed (implying $T_0 = T_{opt}$) and calculate the rms-deviation σ of $B(A)$ as a function of the patchiness parameter p . The result is shown in Fig. 13. We observe that biodiversity remains almost constant for $p < \hat{p}$, i.e., as long as the growth space remains connected. Beyond \hat{p} , however, the species diversity becomes a monotonously increasing function of fragmentation! This finding is in marked contrast to the results presented in Subsection 4.2, where we stated that biodiversity *decreases* as a consequence of environmental deterioration.

Our observation can be explained as follows: within a homogeneous landscape, biodiversity is limited exclusively through competition. Only species with an albedo in the vicinity of the optimal value enjoy a sufficiently large growth rate for survival. And we have shown above that the "window of fitness" is shrinking with increasing irradiation.

In the case of habitat fragmentation, the process

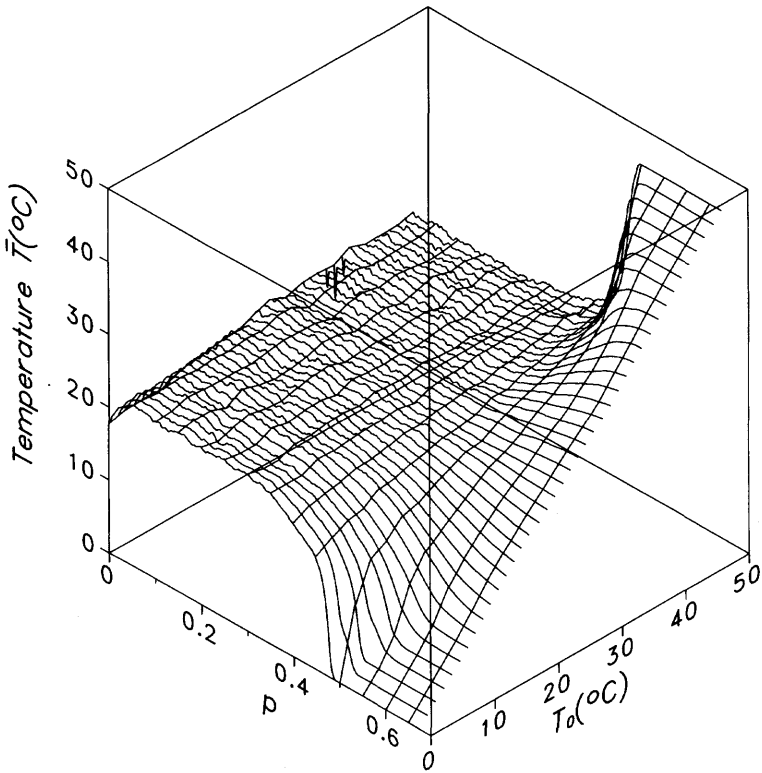


Fig. 12. Bioplanetary temperature \bar{T} as a function of insolation (as represented by T_0) and fragmentation (as represented by p).

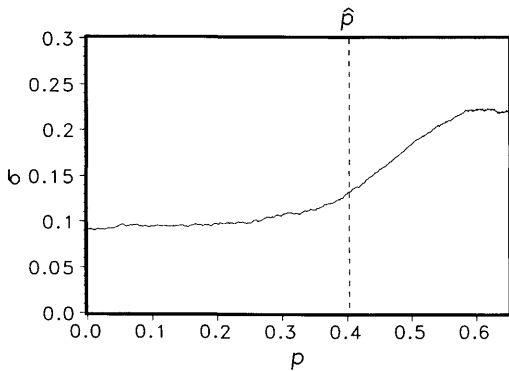


Fig. 13. Growth of biodiversity, expressed by rms-deviation σ of species spectrum $B(A)$, with increasing fragmentation parameter p . $S' = 1$, i.e., $T_0 = T_{opt}$.

of Darwinian competition becomes more and more hampered. The growth space is split up into disconnected “ecological niches” at all scales, where even species with far-from-optimum proper-

ties can subsist. As the relative number of niches grows with p , the biodiversity grows as well.

Yet there is a price to be paid for biodiversity: the overall adaptive capability of the system dramatically decays due to the suppression of the selection process. So Daisyworld becomes more vulnerable to global change the more it becomes egalitarian — biodiversity is harmful from the planetary point of view here!

5.2. Comparison between patchy and trivial reduction of growth space

We want finally to demonstrate that the geometry of the remaining growth space is indeed of paramount importance for the ecological performance of our toy biosphere. To this end, we repeat our simulations for a trivial process of habitat reduction, namely progressive shrinking in time of the rectangular core growth area. The prescription for the process is as follows:

Let $L \geq 2N$ denote the size of the lattice, so the cells (x_j, y_j) of the system obey the inequalities $-L/2 < x_i, y_j \leq L/2$. (36)

Then assume that

$$c(x_i, y_j, t_n) = 0 \text{ if } |x_i| > d/2 \vee |y_j| > d/2, \quad (37)$$

where $d \equiv d(t_n)$, $d(0) = L$, and $d(t_n) \rightarrow 0$ for $t_n \rightarrow \infty$. That means that the habitable zone is a dwindling central square of approximate area d^2 and is a decreasing function of time t_n . The properties of the so-restricted system can be compared to those for the above-described patchy one with identical total growth area, i.e., for

$$p(t_n) = 1 - \left(\frac{d(t_n)}{L}\right)^2 =: \pi. \quad (38)$$

The evolution of the global mean temperature \bar{T} as a function of π under an insolation that corresponds to $T_0 = 30^\circ\text{C}$ is depicted in Fig. 14. Note that, in contrast to the non-trivially fragmented system, the "shrinking square biosphere" is not capable of planetary homeostatic control: \bar{T} increases almost linearly with growing π . This behaviour is approximated by the formula

$$\bar{T}(\pi) = T_0(S)\pi + (1 - \pi)T_{\text{opt}}. \quad (39)$$

The markedly different adaptive capabilities induced by habitat geometry can be explained in a straightforward way. In the 1st case, where the growth area is reduced according to the percolation algorithm, we have approximately $N_1 = pL^2$ non-coverable cells, and almost all of them are adjacent to cells covered by vegetation. In the 2nd

case, where the planetary space decays into a coverable central square and a non-coverable margin, only a very small number of "dead" cells

$$N_2 = 4L(1 - \pi)^{1/2} \ll N_1 \quad (40)$$

are neighbour on a "living" cell. In other words: due to its intricate patchiness, the surface-to-bulk ratio of a percolation cluster is very large in comparison with the surface-to-bulk ratio of a simple square covering the same area! But the size of the surface is an indicator for the total heat flow, which can be activated between the sterile and the fertile zones of Daisyworld. We clearly find that the patchy and lacunary distribution of living cells over the planet is sufficient to suppress "hot spots" via thermal relaxation.

6. Conclusion

Our main objective has been the construction of a 2-dimensional conceptual model for geosphere-biosphere-anthroposphere interaction, which is based on the Lovelock-Watson approach. Our model could be seen as being mid-way between pure toy models and three-dimensional analogical Earth-System models based on state-of-the-art and geographically explicit simulation modules for the atmosphere, the ocean, the biogeochemical cycles, civilisatory land-use etc.

For the sake of computational simplicity, we have designed our extended Daisyworld as an cellular automaton, but this technical option does not affect the validity of our results.

Our system turns out to be rich in exhibiting a number of remarkable phenomena. In particular, we find that spatial heat transport and mutation even improve the self-regulation abilities of the model biosphere. As a matter of fact, in the limit of infinite system size, a 1st-order phase transition from optimum ambient conditions to a non-habitable environment will take place. The existence of a phase transition implies accompanying hysteretic effects, i.e., points of no return.

Fragmentation of potential growth space has a significant influence on the homeostatic performance of the biosphere. A unique threshold can be identified, where the regulation of global temperature becomes inhibited due to habitat disconnection. We also find that an unrestricted Darwinian selection of species under deteriorating environ-

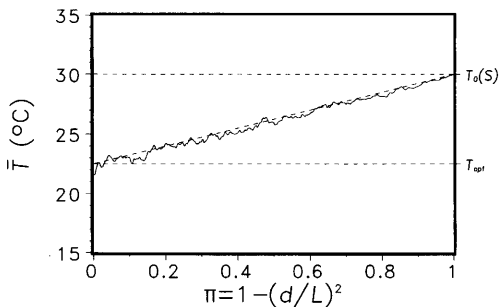


Fig. 14. Variation of global mean temperature \bar{T} with progressive trivial shrinkage of habitable area. As in Fig. 9, S' has been chosen to generate $T_0(S') = 30^\circ\text{C}$. The tilted broken line indicates the linear estimation as expressed in eq. (39).

mental conditions warrants the subsistence of the biosphere as a whole. Biodiversity benefits from fragmentation, yet reduces the overall ecological performance of Daisyworld.

We plan to further pursue our simple geophysiological approach to Earth-system analysis by incorporating additional elements into our model. The next steps will be to include caricatures of the hydrological and biogeochemical cycles. Another interesting option is to simulate civilisatory habitat

fragmentation by more realistic processes for urbanization and infrastructure expansion.

7. Acknowledgements

The authors wish to thank K. Hasselmann and J. Lovelock for a critical reading of the manuscript and valuable comments. Work has been supported by IBM Deutschland through Studienvertrag H009.

REFERENCES

- Bolin et al. 1996. *Climate Change 1995. The IPCC Second Assessment Report*. Cambridge University Press, Cambridge.
- De Gregorio S., Pielke, A. and Dalu, G. A. 1992. Feedback between a simple biosystem and the temperature of the earth. *J. Nonlinear Sci.* **2**, 263–292.
- Goles, E. (ed.) 1994. *Cellular automata, dynamical systems and neural networks*. Kluwer acad. Pub., Dordrecht.
- Henderson-Sellers A. and McGuffie, K. 1990. *A climate modelling primer*. John Wiley & Sons, Chichester.
- IGBP, 1994. IGBP in action: work plan 1994–1998. IGBP report 28. The International Geosphere-Biosphere Programme. *A study of global change (IGBP) of the International Council of Scientific Unions (ICSU)*, Stockholm.
- Isakari and Somerville, R. C. J. 1989. Accurate numerical solutions for Daisyworld. *Tellus* **41B**, 478–482.
- Lovelock, J. E. 1989. *The ages of Gaia*. Oxford University Press, Oxford.
- Lovelock, J. E. 1991. *GAIA — the practical science of planetary medicine*. GAIA Books, London.
- Ott, E., Sauer, T. and Yorke, J. A. 1994. *Coping with chaos*. Wiley Series in Nonlinear Science, John Wiley & Sons, New York.
- Saunders, P. T. 1994. Evolution without natural selection. Further implications of the Daisyworld parable. *J. Theor. Biol.* **166**, 365–373.
- Schellnhuber, H. J. and Von Bloh, W. 1994. Homöostase und Katastrophe. In: *Klimaänderung und Küste* (eds. Schellnhuber, H. J. and Sterr, H.) Springer, Berlin, 11–27.
- Schellnhuber, H. J. (ed.) 1997. *Earth system analysis: integrating science for sustainability*. Springer Verlag, Berlin, to appear.
- Schuster, H. G. 1989. *Deterministic chaos: an introduction*. Verlag Chemie, Weinheim.
- Stauffer, D. 1985. *Introduction to percolation theory*. Taylor and Francis, London.
- Walter, H. and Breckle, S.-W. 1991. *Ökologie der Erde*, vol. 1–4. Gustav Fischer Verlag, Stuttgart.
- Watson, A. J. and Lovelock, J. E. 1982. The regulation of carbon dioxide and climate. Gaia or geochemistry? *Planet. Space Sci.* **30**, 793–802.
- Watson, A. J. and Lovelock, J. E. 1983. Biological homeostasis of the global environment: the parable of Daisyworld. *Tellus* **35B**, 286–289.
- WCRP (World Climate Research Programme), 1994. *Draft of the WCRP long-term plan, 1996–2005*.
- Wolfram, S., 1986. *Theory and applications of cellular automata*. World Scientific, Singapore.
- Zeng, X., Pielke, R. A. and Eykholt, R. 1990. Chaos in Daisyworld. *Tellus* **42B**, 309–318.